Jefferson Lab
E94010 Technical Note
March 22, 2001

Dependence of the Cross-Section on Acceptance Cuts for E94010 v. 1.2

K. Slifer
Temple University
Philadelphia, PA 19122

E-mail
slifer@jlab.org

Contents

1 Introduction

As first pointed out in the November 30, 2000 collaboration meeting, there is a large dependence of the experimental cross-section on the sector of the acceptance that is selected. Fig. 1 shows the variation of the 2 GeV cross-section as the acceptance cut is gradually relaxed from $\phi_t \leq$15 mrad,$\theta_t \leq$ 30 mrad to $\phi_t \leq$40 mrad,$\theta_t \leq$60 mrad. Here ϕ_t refers to the horizontal scattering angle, θ_t refers to the vertical angle. Both angles are taken with reference to the central spectrometer ray.

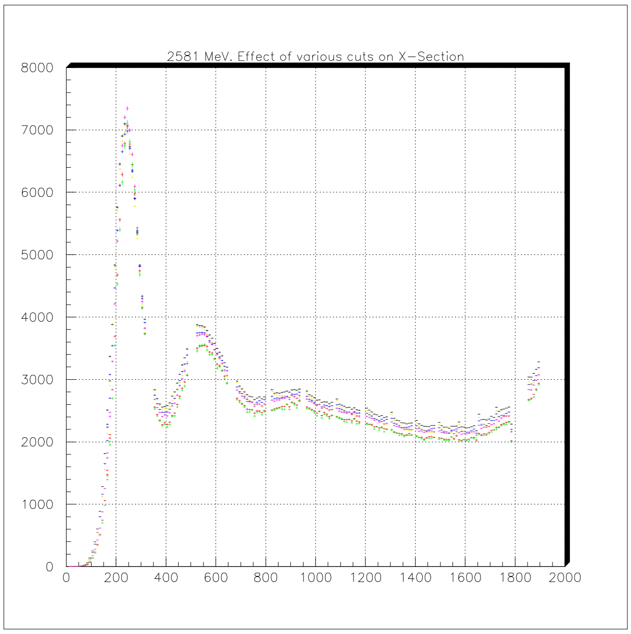

Figure 1: 2 GeV Cross-Section

To determine the cause of the variation, we have examined the ability of the acceptance simulation to reproduce target quantities*. We then use this information to select a range where the cross-section will be stable to variations in the cut limits.

In all that follows, a particle ID cut of the type discussed in [2] is used. There is no shift applied to either the data or simulation variables, and all results apply exclusively to the Electron Arm Spectrometer.

2 Comparison of Data and Acceptance Simulation

2.1 Carbon Data

To study the agreement of the simulated acceptance and experimental data, we first looked at scattering from thin carbon foils. The foils were evenly spaced along the beam line at

*For an independent, earlier study see A. Deur [1]

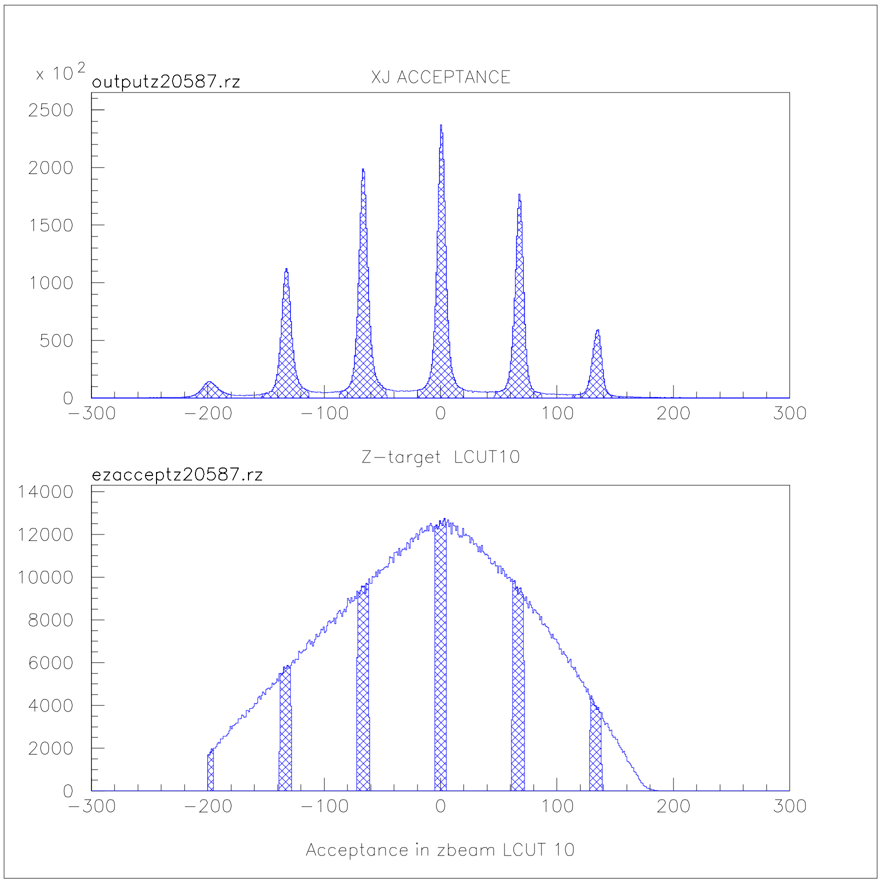

Figure 2: Carbon data Z_{beam} distribution. The top panel shows the experimental Z_{beam} cut while the lower panel shows the cut on the acceptance.

intervals of 6.67cm. For this study, each of the carbon foils is selected in turn, (see Fig. 2), then we check the agreement between experiment and simulation for ϕ_t. The comparisons done in this study are all relative. A Mott dependence has been added to the simulation in order to make the comparison.

The spectrometers were moved briefly to take elastic data during E94010 and then returned to their nominal angle of approximately 15.5 degrees. To ensure that there is no systematic difference between the two periods, we look at data taken before the move and after. Fig. 3 shows the result for an incident energy of 862.0 MeV before the spectrometer is moved. Fig. 4 shows the result for an incident energy of 2580.5 MeV after the spectrometer has been moved. As expected the central foils are reproduced best by the acceptance simulation, with agreement not so good for the outer foils. A shift between experiment and simulation can be seen in the ϕ_t distribution.

Unexpectedly, the central foil (#4) agreement is not good for the 862.0 MeV run. We conclude that the simple Mott dependence introduced into the acceptance for this study is insufficient to reproduce the physics variation for this near elastic run.

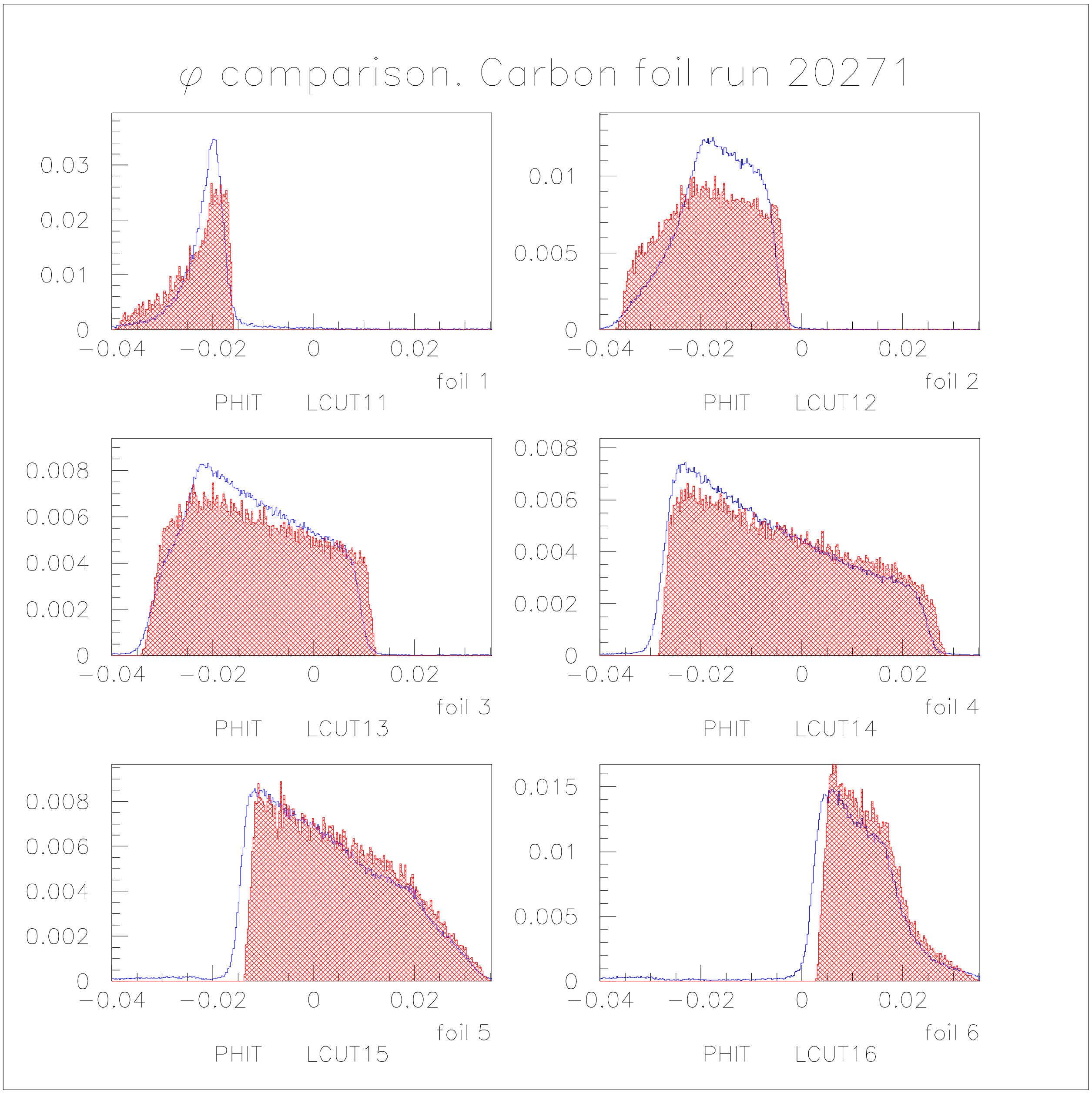

Figure 3: Carbon Data ϕ_t before move.E_0=862.0 MeV. P_0 =823.3 MeV/c. Foil #4 is the central foil.

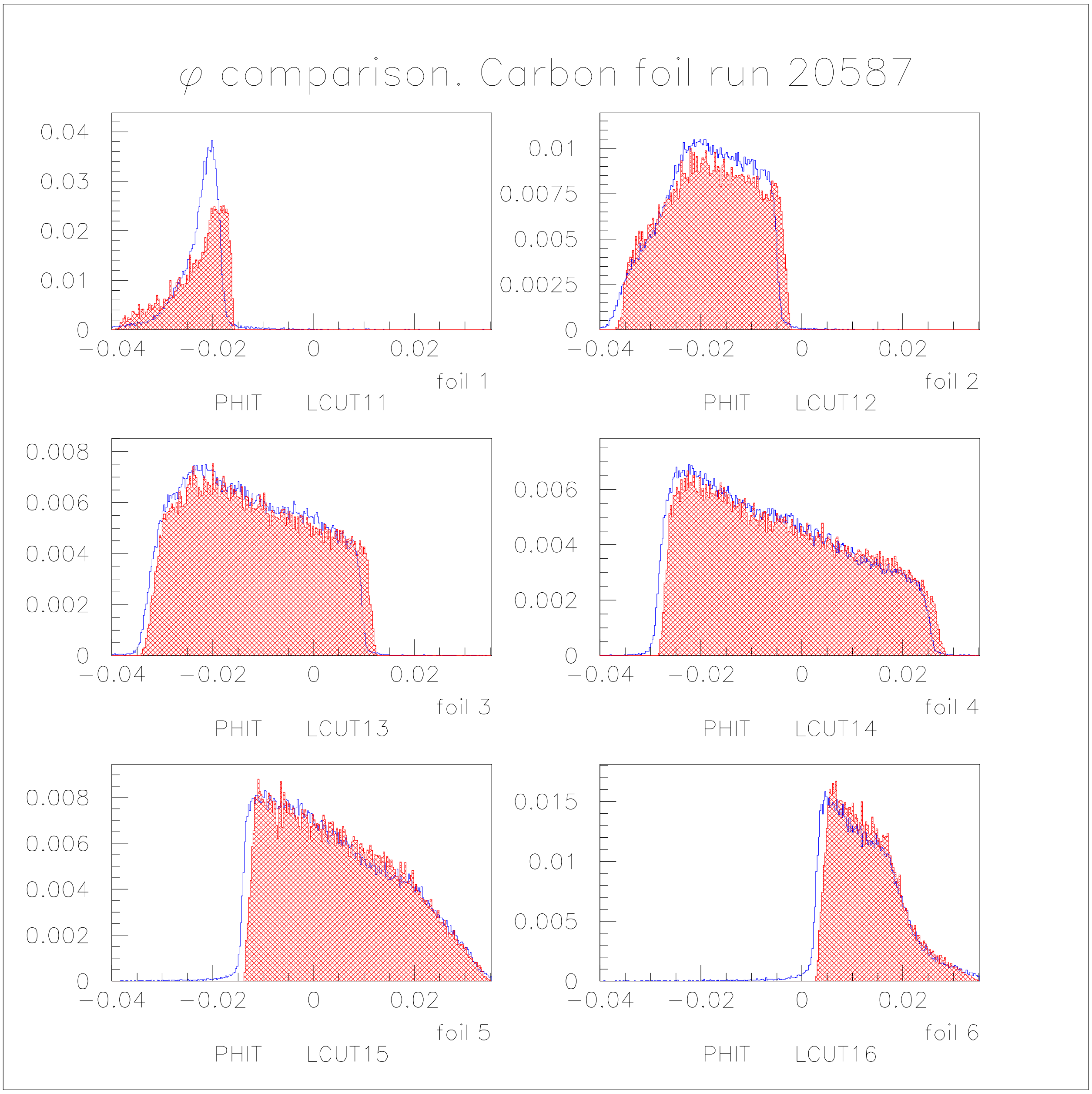

Figure 4: Carbon Data ϕ_t after move. E_0 = 2580.5 MeV. P_0 = 2273.0 MeV/c. Foil #4 is the central foil.

2.2 ^{3}He data

To check the conclusion of the previous section, we investigate the ability of the acceptance to reproduce the four target quantities y_t, ϕ_t, δp/p, and θ_t for a ^{3}He run before the move, 2698, and for a ^{3}He run after the move, 3393. These two runs are chosen because they contain data taken at large energy loss ν, where the physics variation across the acceptance should be adequately described by a Mott dependence. Run 2698 is a 5 pass run with E_0 =4238.6 MeV and P_0 = 1755.9 MeV which was dedicated specifically to acceptance studies. Run 3393 is a 6 pass run with E_0 = 5058.2 MeV and P_0 = 2609.2 MeV.

2.2.1 Foil-like cuts

Figs. 5 and 6 show the ϕ_t comparison after selecting data from 6 different locations along the ^{3}He target length at the location of the foil placement from the previous section. For example the middle right panel shows ϕ_t for a 4 cm. target region centered about z=0. The bottom left shows a 4 cm. slice centered at z=+6.67 cm. etc. We note that the central target region ϕ_t distribution is well reproduced for both periods.

There is no systematic ϕ_t shift as is observed in the carbon data. However the simulation falls off too soon in the negative ϕ_t region compared to the data. This explains the behavior of Fig. 1. When the cuts are relaxed, we accept data from large negative ϕ_t. In this region, the cross-section grows unreasonably when the data is normalized by the acceptance weight.

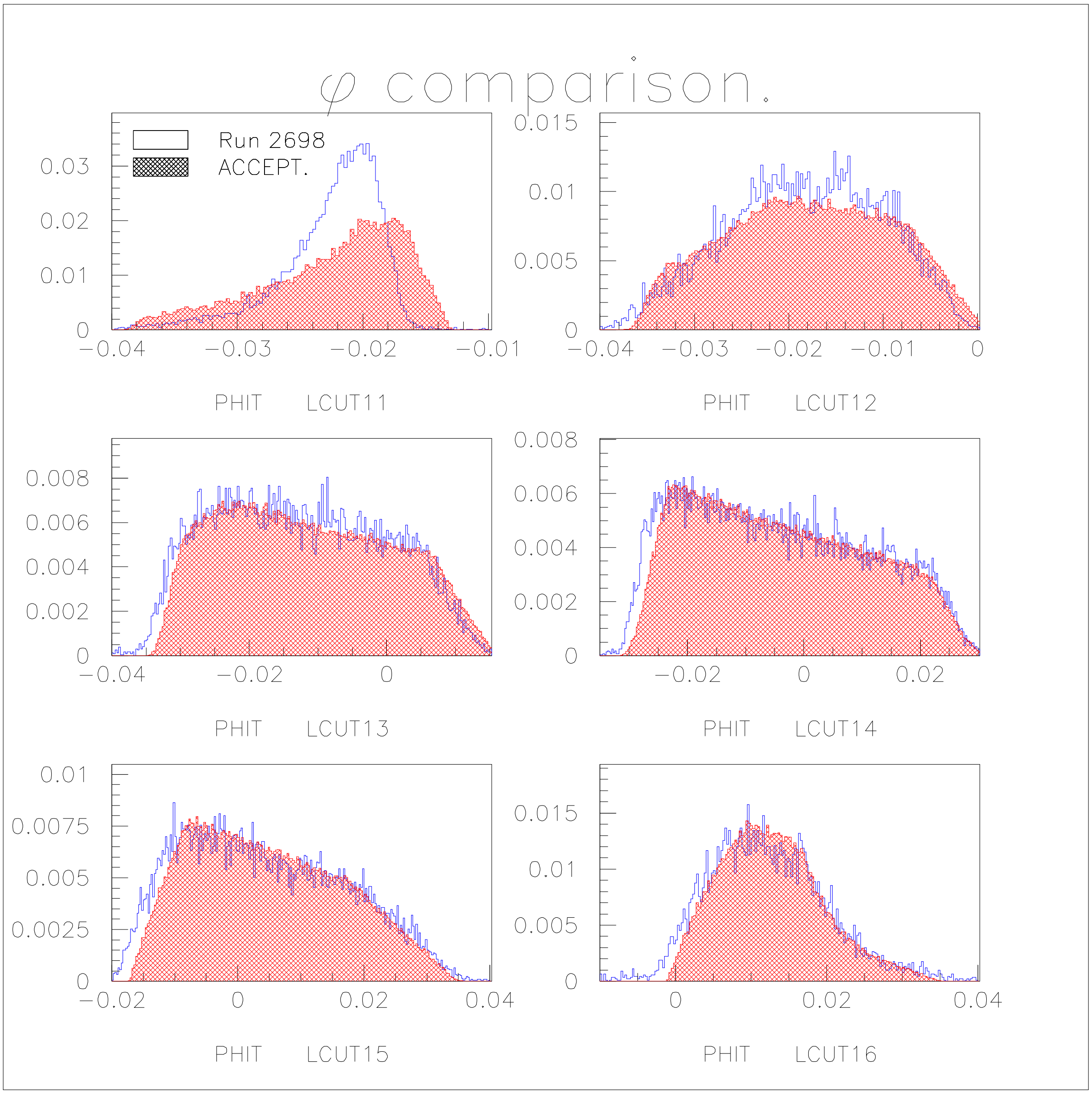

Figure 5: ^{3}He Data ϕ_t before move. E_0 = 4238.6 MeV. P_0 = 1755.9 MeV/c. Each panel represents a 4cm target slice at intervals of 6.67cm along the target length. The middle right panel shows events centered at z=0.

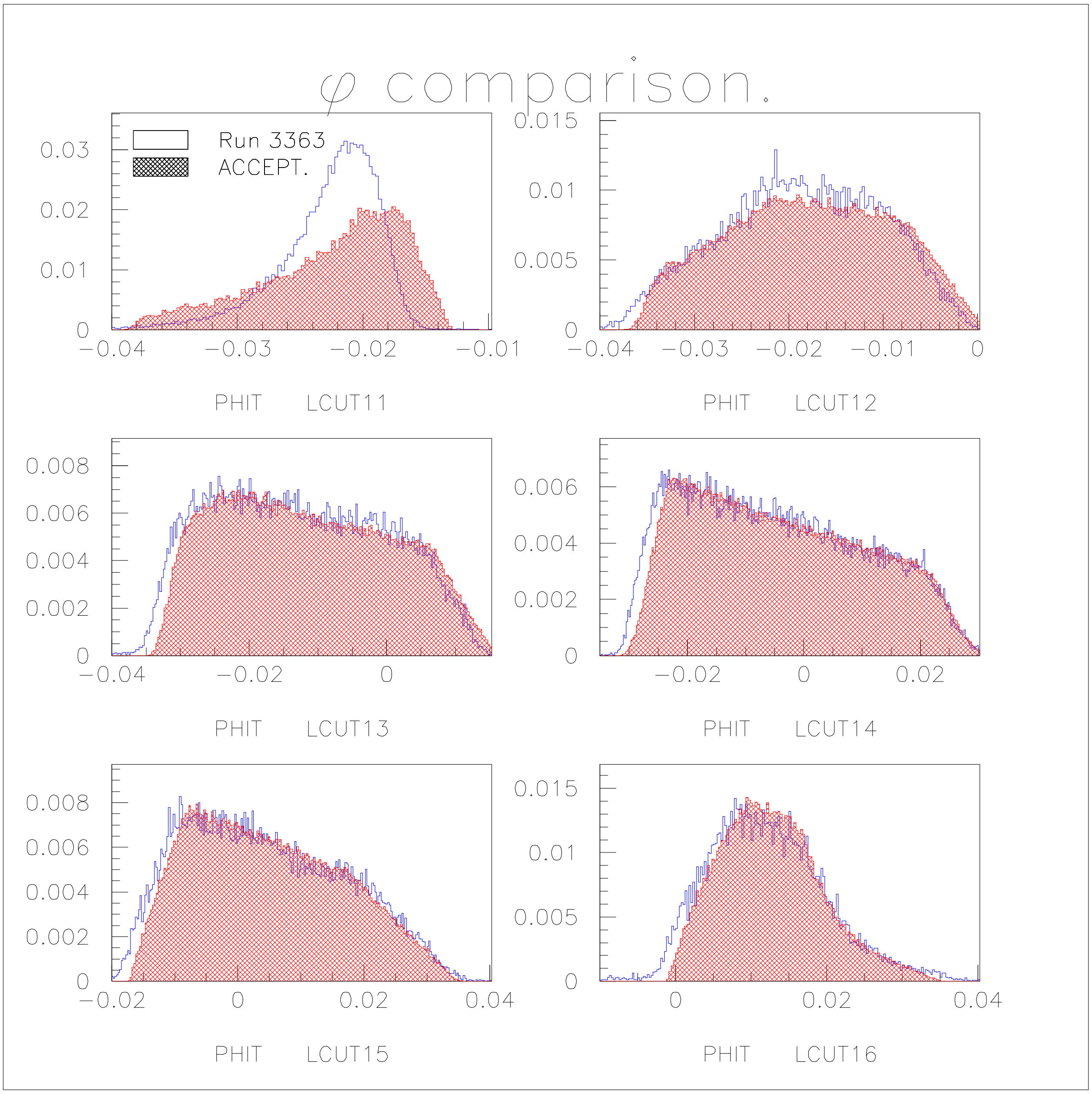

Figure 6: ^{3}He Data ϕ_t after move. E_0 = 5058.2 MeV. P_0 = 2609.2 MeV/c. Each panel represents a 4cm target slice at intervals of 6.67cm along the target length. The middle right panel shows events centered at z=0.

2.2.2 12 cm. target

Since the ϕ_t agreement is best near the target center, we next choose a z_{beam} cut of $\pm$ 6 cm. corresponding to a target length of 12 cm. This choice of target length also presents the advantage that it nearly coincides with the portion of the target polarization that was sampled by the NMR pickup coils. Now we look at several target quantities in order to determine where the agreement is acceptable and where there will be discrepancies. **NOTE: The y_t distributions in the following graphs have been reversed compared to the raw data. That is, positive y_t corresponds to downstream.**

Both δp/p and θ_t are reproduced quite well, within reasonable limits. The ϕ_t agreement is good for $\phi_t \geq$ -15 mrad. The y_t plot shows the asymmetric effect that the collimator has on either side of the scattered electron distribution. On the upstream side the collimator primarily blocks events with a scattering angle larger than the central angle. There are fewer events at a larger scattering angle due to the cross-section drop-off so we don't see the effect of the collimator as much. On the downstream side, the collimator primarily blocks events scattered at a smaller angle than the central angle. Since the event rate is larger at smaller angle the collimation is more noticeable.

It is apparent that the y_t distribution is reproduced well only on one side. We can not say for certain which since the comparison is relative. (The simulation normalization could just as easily been chosen to agree with the negative y_t data as with the positive). This does not really indicate a problem with the simulation as there are no cuts on ϕ_t, θ_t applied here. Reasonable cuts will eliminate events that deviate very much from the central ray and which are affected most by the collimator. The next section supports this conclusion.

We note that there is no large systematic difference seen between the period before the move and after.

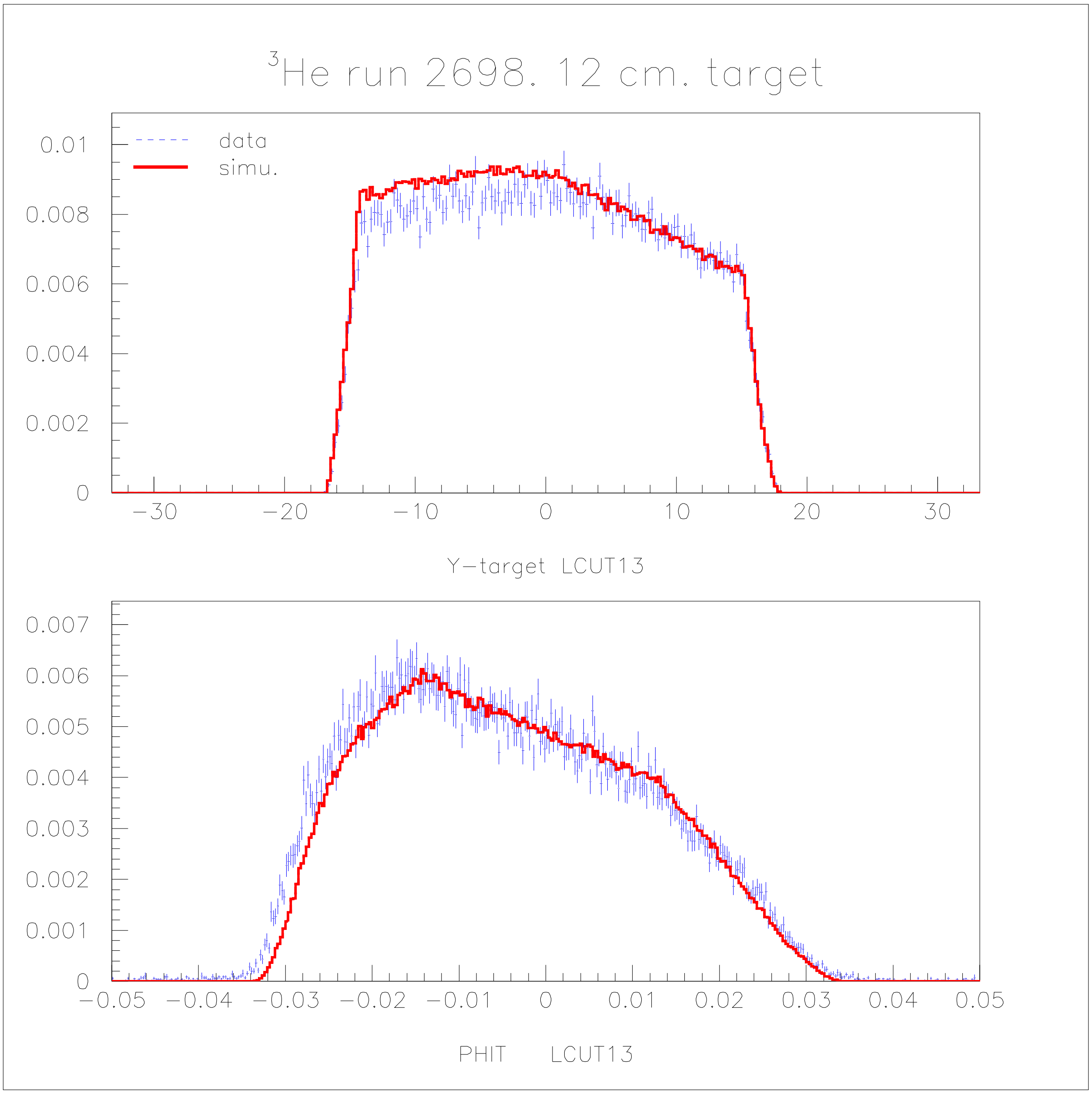

Figure 7: ^{3}He Data ϕ_t before move. E_0 =4238.6 MeV. P_0 = 1755.9 MeV/c . Positive y_t corresponds to downstream events in this plot.

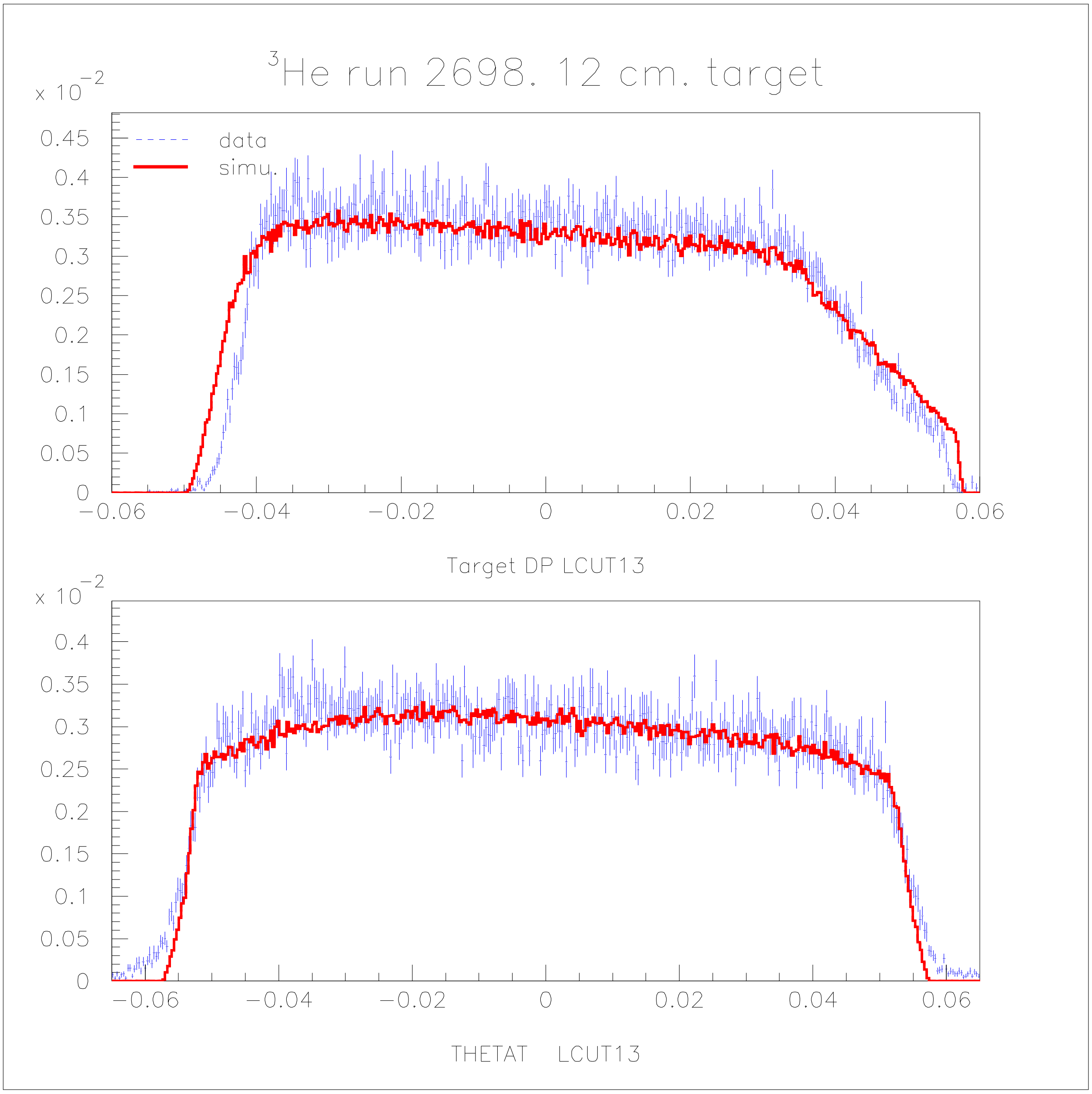

Figure 8: ^{3}He Data ϕ_t before move. E_0 =4238.6 MeV. P_0 = 1755.9 MeV/c

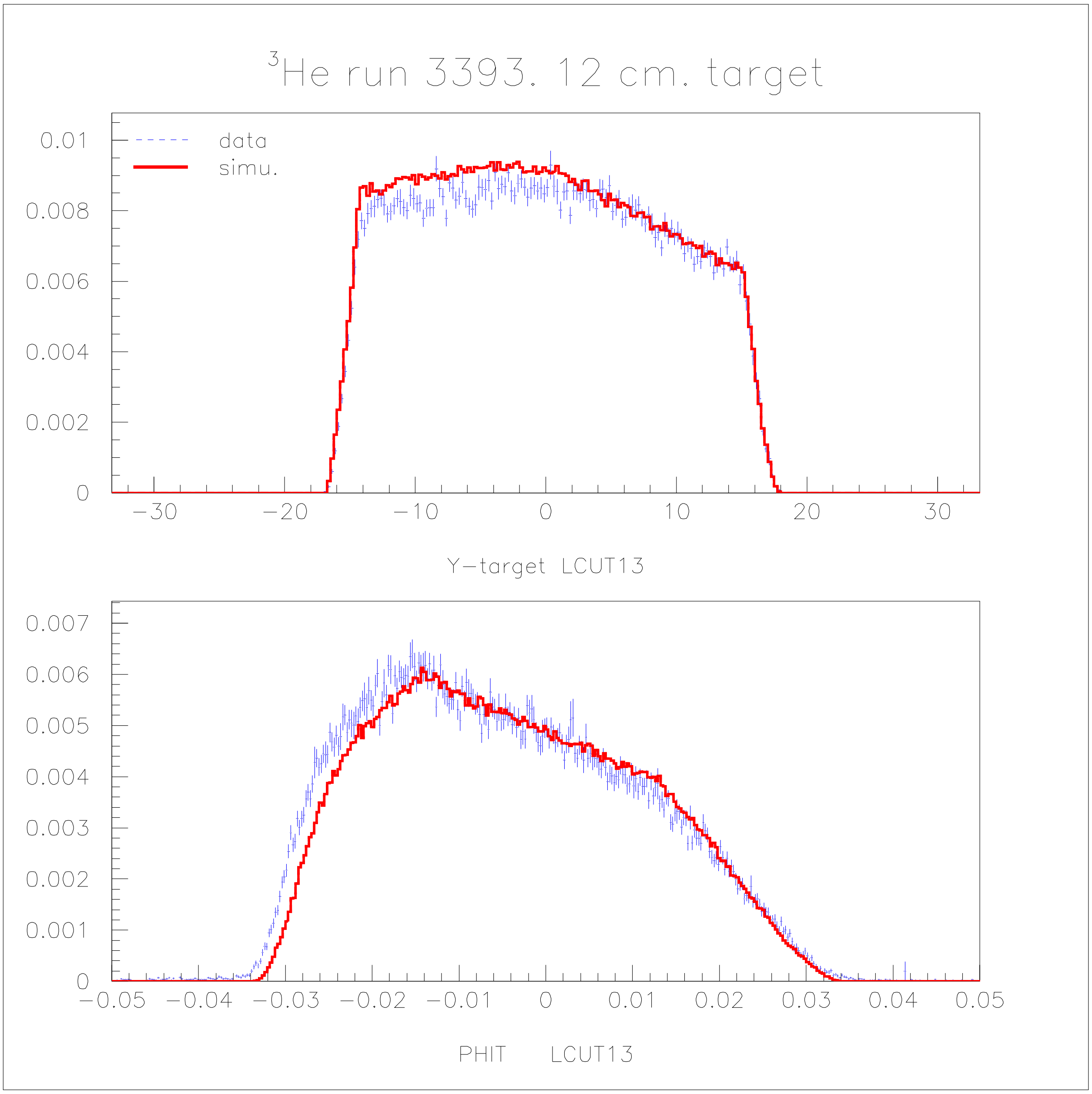

Figure 9: ^{3}He Data ϕ_t after move. E_0 = 5058.2 MeV. P_0 = 2609.2 MeV/c . Positive y_t corresponds to downstream events in this plot.

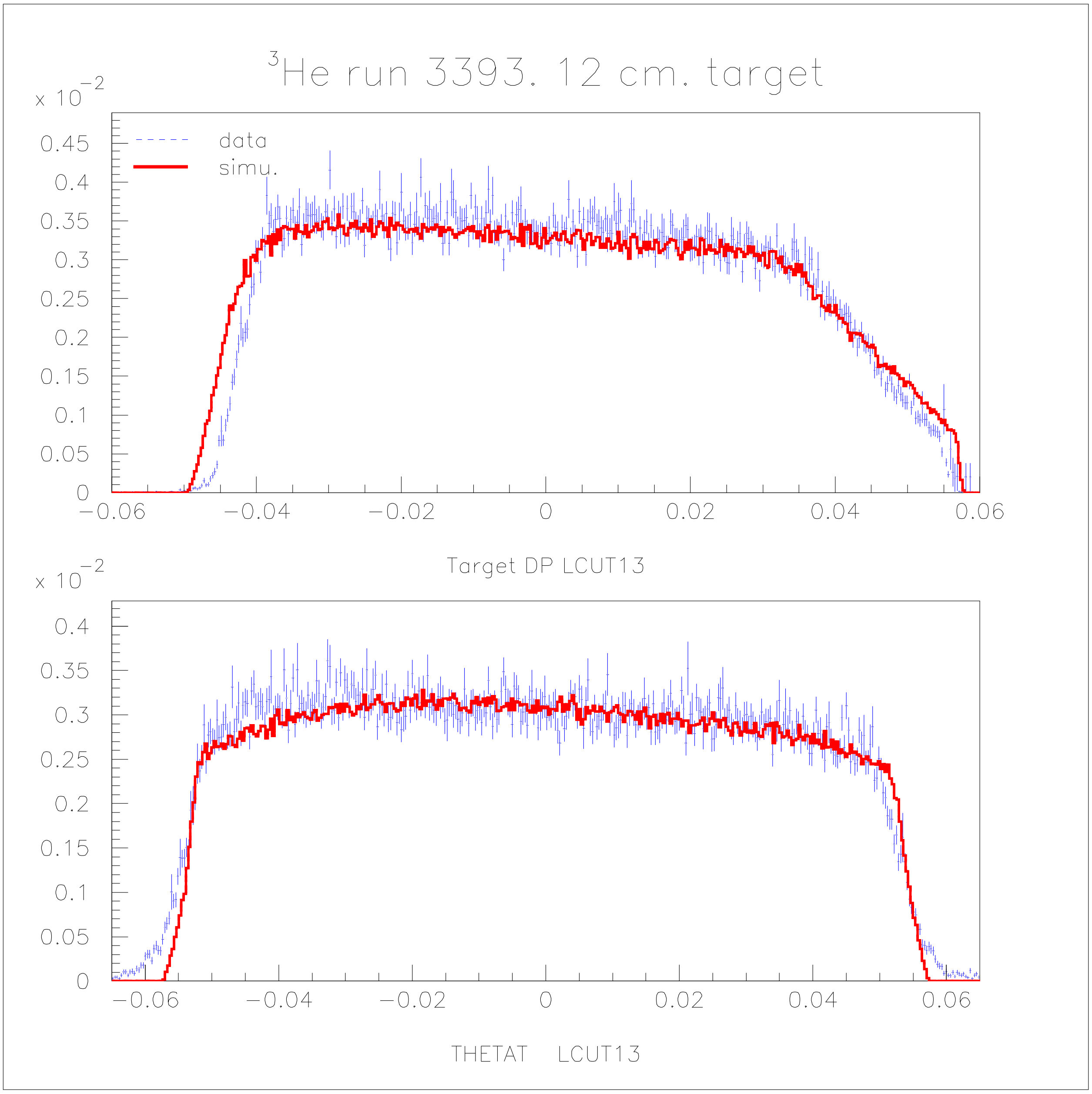

Figure 10: ^{3}He Data ϕ_t after move. E_0 = 5058.2 MeV. P_0 = 2609.2 MeV/c

3 Stability of the Cross-Section to Cut Variation

Using the results of the previous sections we can now select a final cut on the acceptance where the simulation should reasonably reproduce the data. A two-dimensional y_t, ϕ_t cut (see Fig. 11) is included as suggested in [3] to avoid the edge of the acceptance.

The resulting cross-sections for an incident energy of 3381 MeV are shown in Fig. 12 and Fig. 13. The effect of further increasing the limits is shown in Fig. 14 and Fig. 15. For large energy loss all the cross-sections agree within the statistical error. However, at small ν a definite systematic variation is observed as the θ_t and ϕ_t limits are relaxed. The Quasi-Elastic peak is most susceptible to variation, with shifts greater than 10% for the extreme low ν side. (Note that these differences exceed the range of the graph.)

We conclude that for a 12cm target we can not exceed a ϕ_t of $\pm$ 15 mrad and a θ_t of $\pm$ 30 mrad.

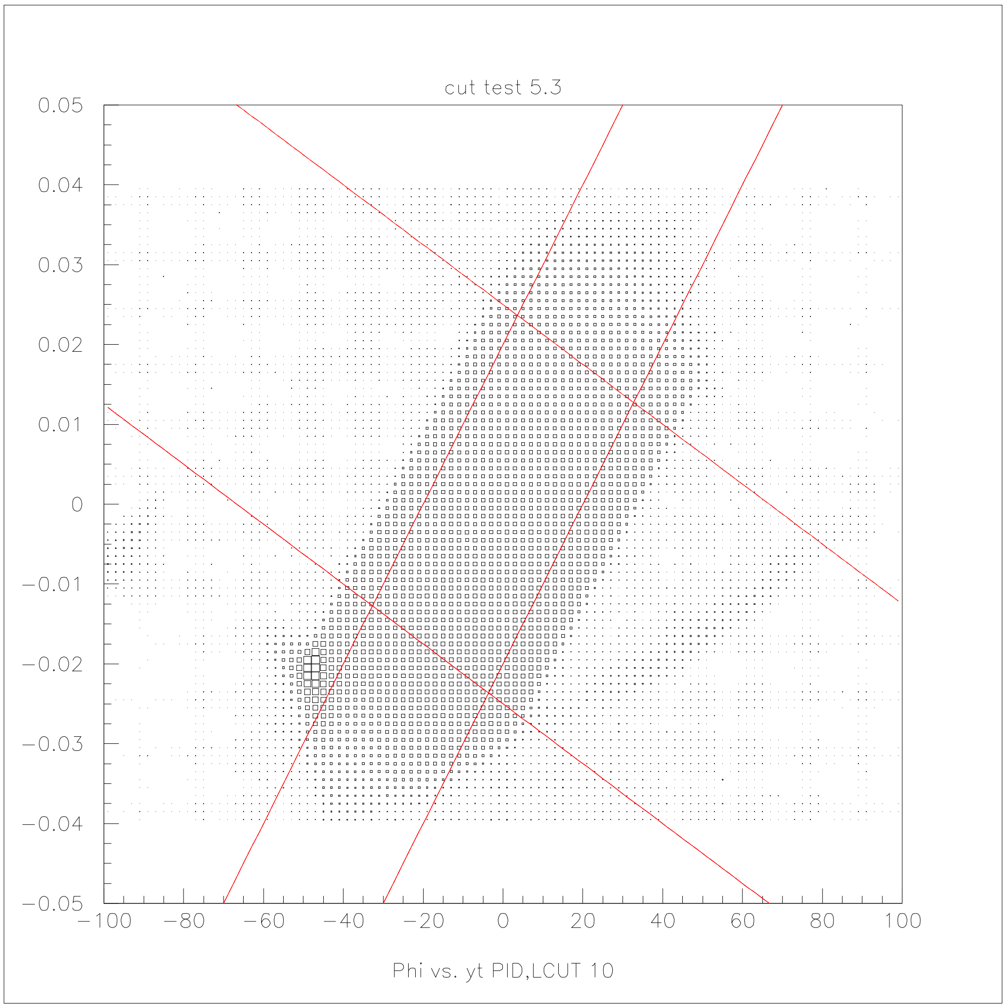

Figure 11: ϕ_t vs. y_t. Positive y_t corresponds to downstream events in this plot.

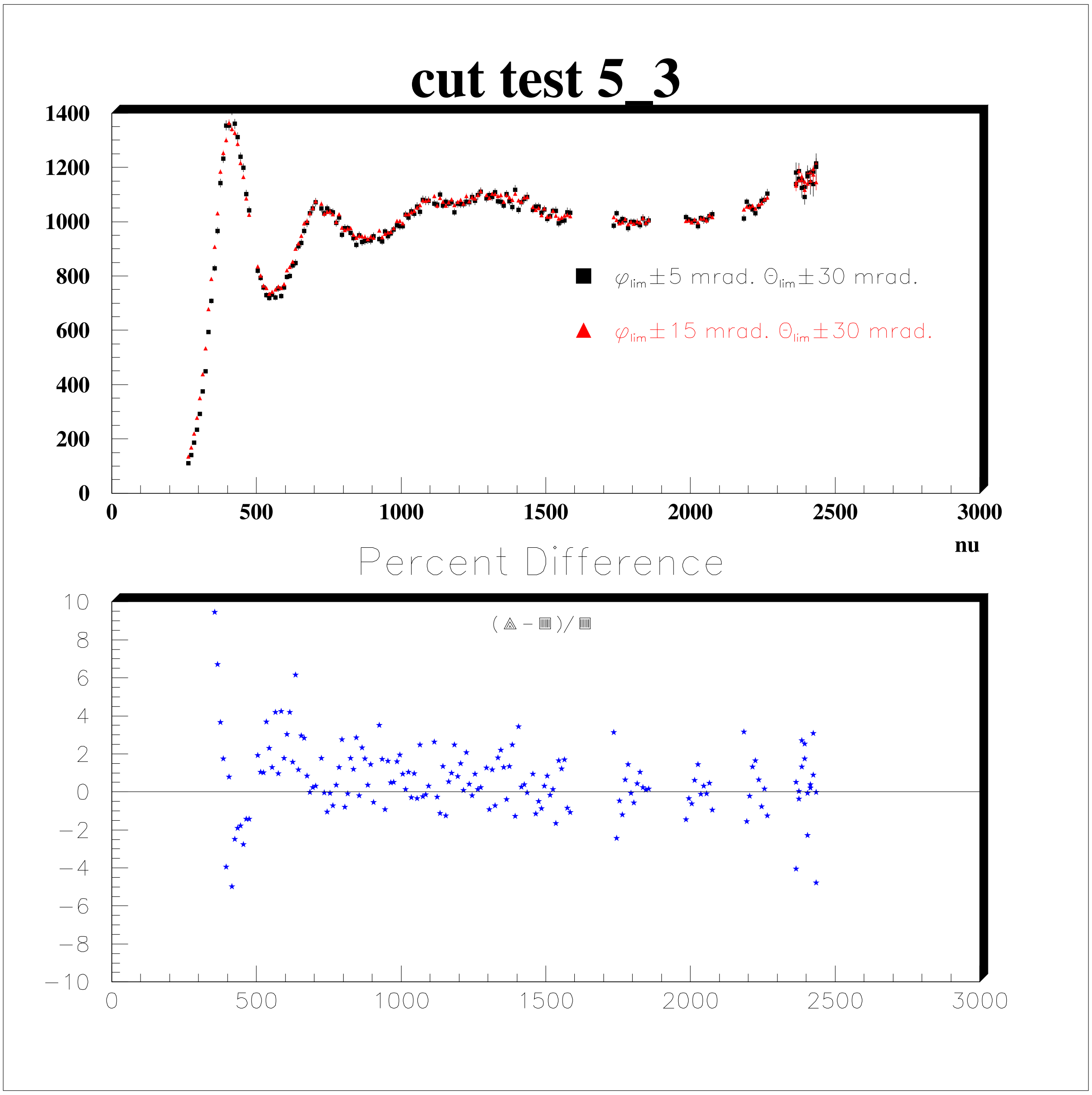

Figure 12: 3 GeV X-Section. **Top:** Cross-section variation as the ϕ_t cut is relaxed from ± 5 mrad to ± 15 mrad, and the θ_t cut is held constant at ± 30 mrad. **Bottom:** Percent difference between the two cross-sections.

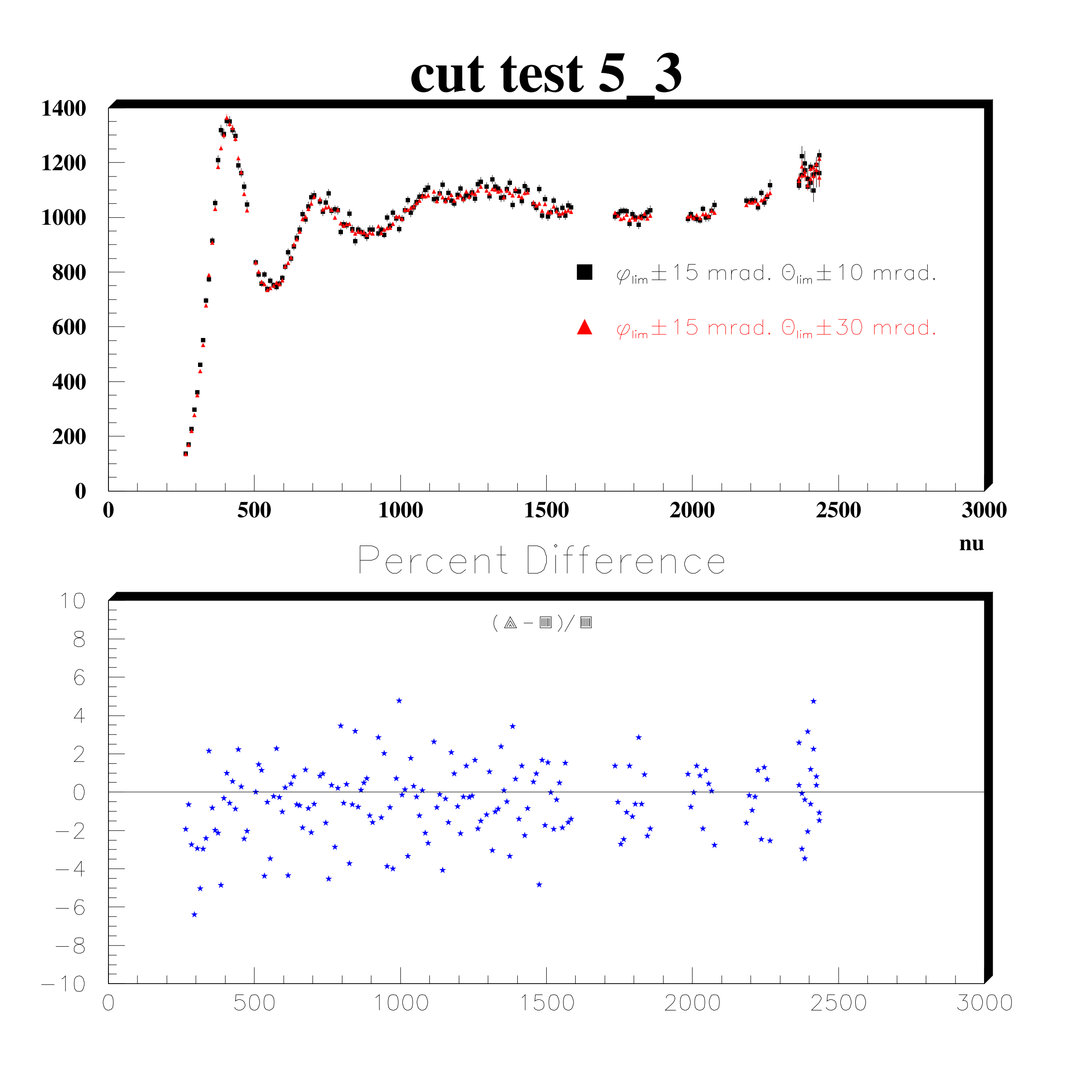

Figure 13: **Top:** Cross-section variation as the θ_t cut is relaxed from ±10 mrad to ±30 mrad, and the ϕ_t cut is held constant at ±15 mrad. **Bottom:** Percent difference between the two cross-sections.

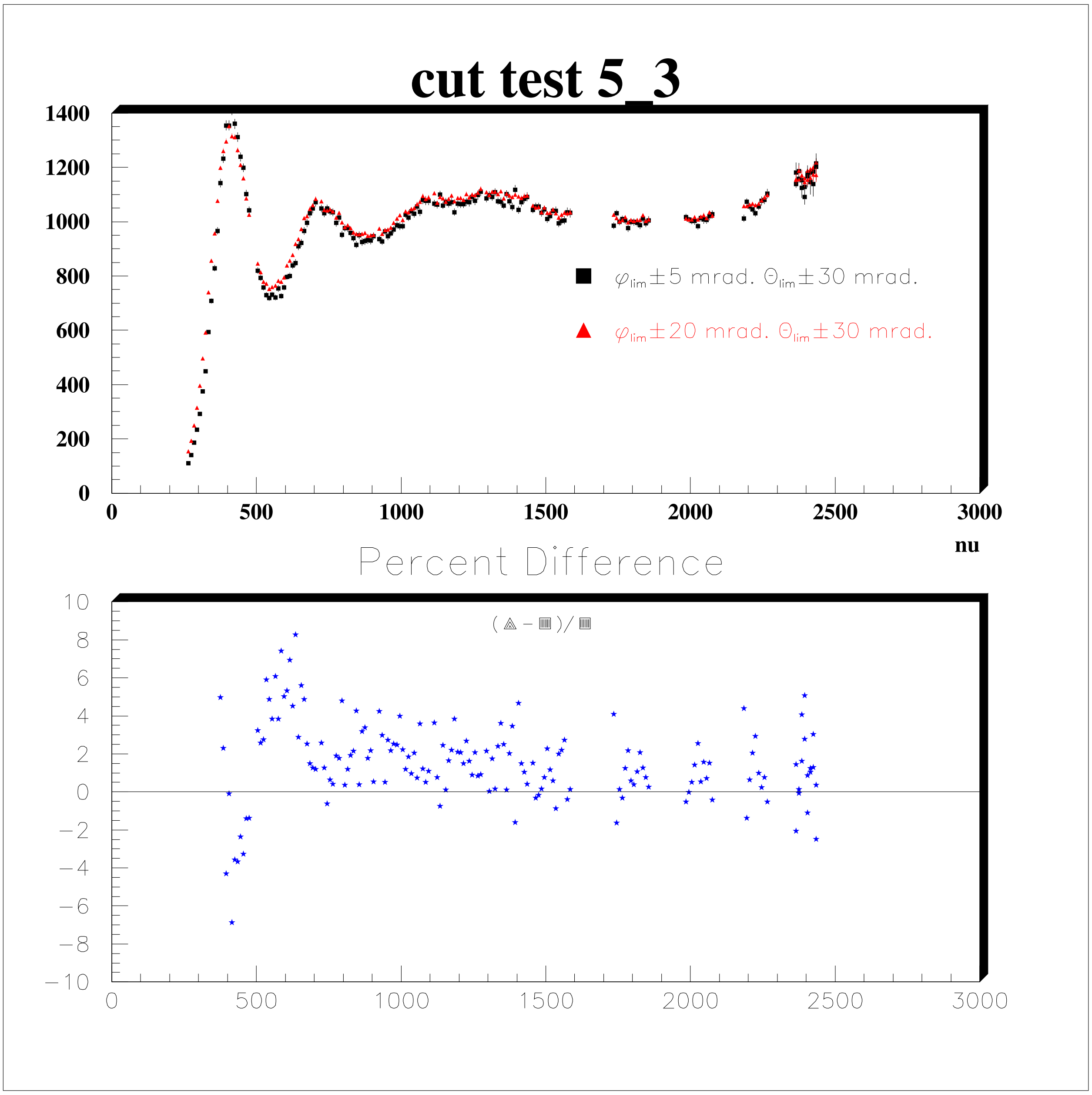

Figure 14: **Top:** Cross-section variation as the ϕ_t cut is relaxed from ± 5 mrad to ± 20 mrad, and the θ_t cut is held constant at ± 30 mrad. **Bottom:** Percent difference between the two cross-sections.

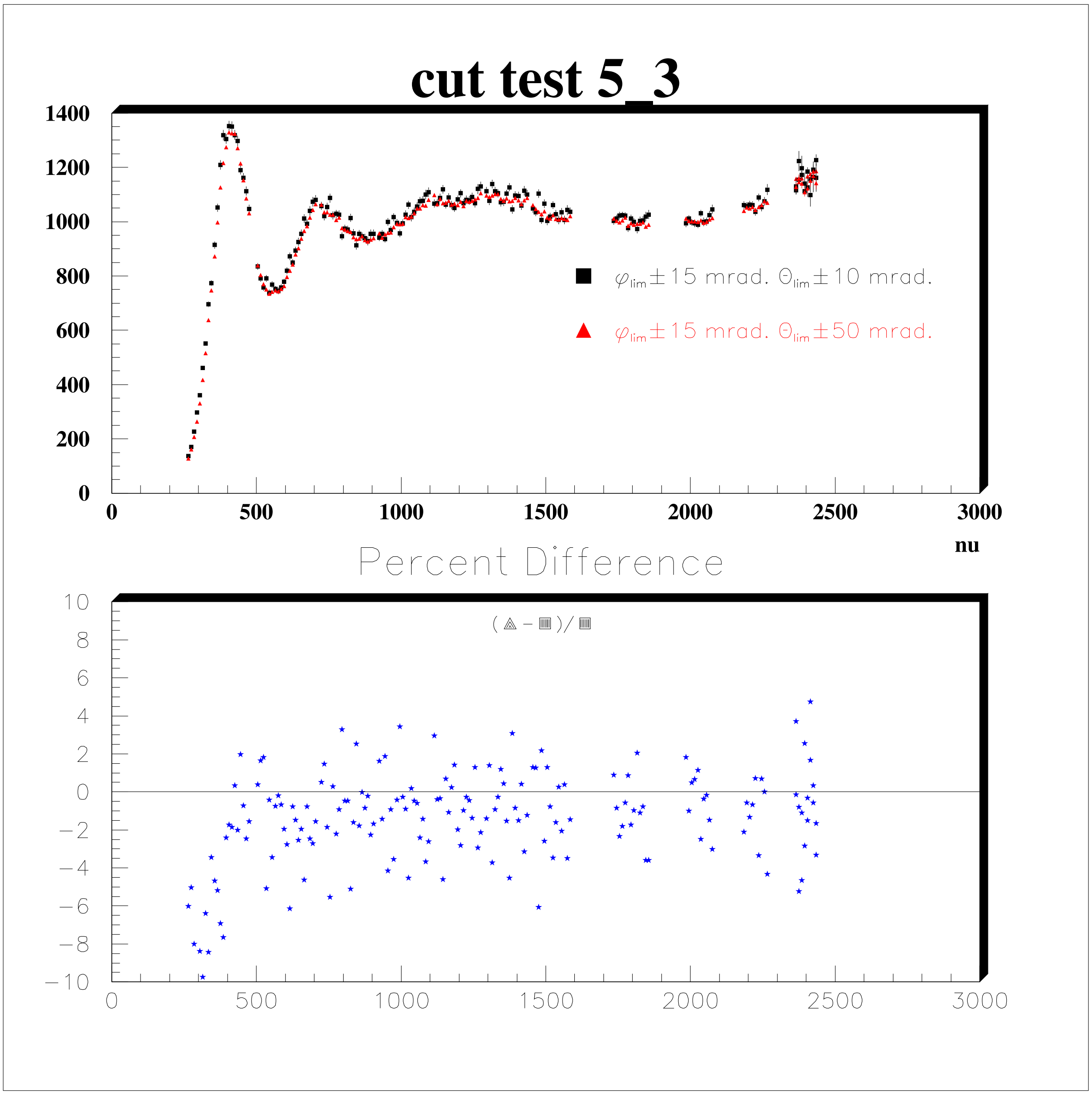

Figure 15: **Top:** Cross-section variation as the θ_t cut is relaxed from ± 10 mrad to ± 50 mrad, and the ϕ_t cut is held constant at ± 15 mrad. **Bottom:** Percent difference between the two cross-sections.

4 Final Comparison of Target Variables

To complete the study, we look at the simulation agreement after the final cut has been applied. Figs. 16, 17 show the comparison. Here, the data has been taken at a central ν of 2400 MeV (the last set of data points in the 3 GeV cross-section).

The agreement is good, except for $\delta p/p$ at the edges. This presents no problem as the edges can be removed by a cut on the cross-section variable ν.

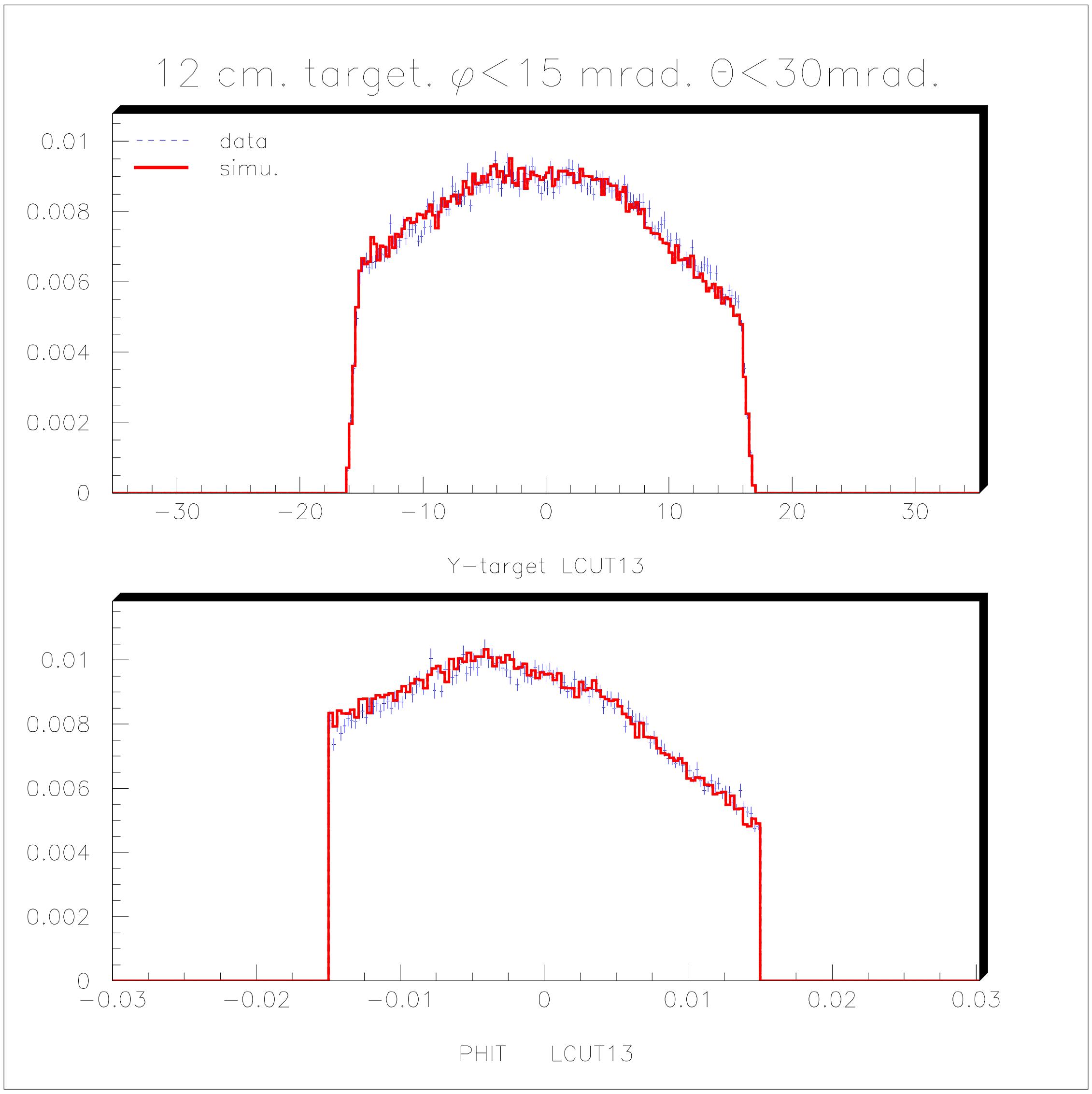

Figure 16: ^{3}He Data target variables with final cut. Positive y_t corresponds to downstream events in this plot.

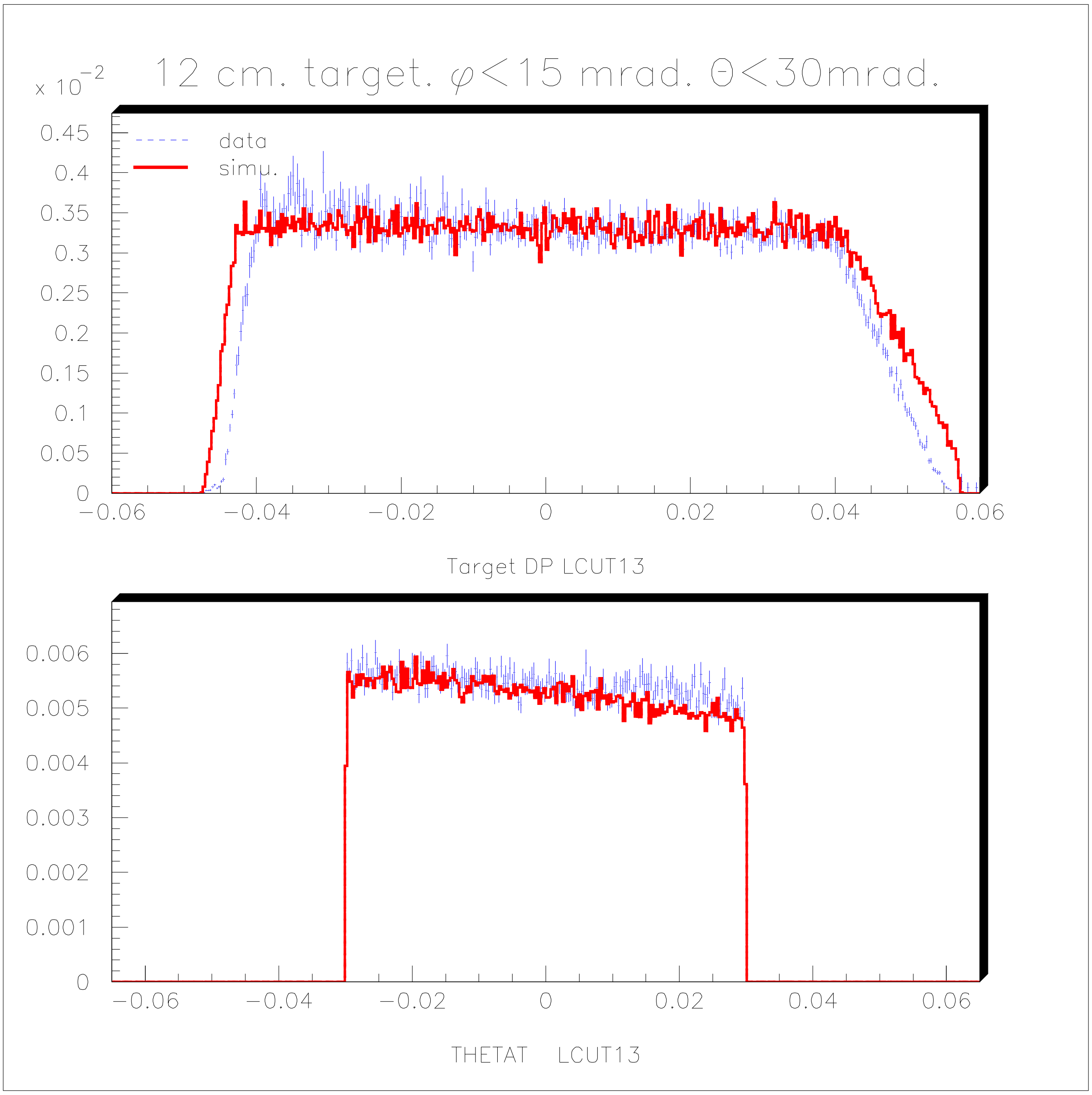

Figure 17: ^{3}He Data target variables with final cut

5 Conclusion

We have shown that the cross section for a 12 cm target is stable to variations in the acceptance cut within the rage -15 mrad $\leq \phi_t \leq$ 15 mrad and -30 mrad $\leq \theta_t \leq$ 30 mrad. Outside of this range, the cross section can vary significantly depending on the range selected.

For convenience, we list the complete analysis cut:

- -15 mrad $\leq \phi_t \leq$ +15 mrad
- -30 mrad $\leq \theta_t \leq$ +30 mrad
- -6cm $\leq Z_{beam} \leq$ +6cm.
- abs(ϕ_t - 0.375y_t) $\leq$ 0.025
- abs(ϕ_t + y_t)$\leq$0.020
- PID cut

6 Acknowledgements

I'd like to thank Nilanga Liyanage and Seonho Choi for valuable discussions on the topic of this note.

References

[1] A. Deur, "*Acceptance Simulation Studies for the Hall A High Resolution Spectrometers.*" E94010 Technical Note. (Nov, 2000).

[2] K. Slifer, "*Shower Detector Calibration and Cut Optimization for E94010*", E94010 Technical Note. (May 2000).

[3] N. Liyanage, "*Study of systematic uncertainties for cross-section measured in E94-010*", E94010 Technical Note. (March,2001)